

Microstructure comparison of ZK60 alloy under casting, twin roll casting and hot compression

WANG Shou-ren(王守仁)¹, WANG Min(王敏)², KANG Suk-bong³, CHO Jae-hyung³

1. School of Mechanical Engineering, University of Ji'nan, Ji'nan 250022, China;

2. School of Materials Science and Engineering, Shandong University, Ji'nan 250022, China;

3. Korea Institute of Materials Science, 66 Sangnam-dong, Changwon 641010, Korea

Received 25 March 2009; accepted 4 September 2009

Abstract: The microstructures of ZK60 alloy under conventional direct as-casting (DC), twin roll casting (TRC) and twin roll casting followed by hot compression (TRC-HC) were analyzed by optical morphology (OM), electron backscatter diffraction (EBSD) and X-ray diffraction (XRD). The deformation condition of hot compression is 350 °C, 0.1 s⁻¹. The microstructural evolution under TRC-HC deformation followed by annealing at different temperatures and time was discussed. The results show that TRC provides more modified microstructure compared with DC. Twins are found in TRC processing; dynamic recrystallization (DRX), shear bands and twins are found in TRC-HC. A short annealing time has little effect on hardness, while during a long time annealing, it is found that low annealing temperatures increase the micro-hardness and high temperature decreases it.

Key words: microstructural evolution; anneal; dynamic recrystallization; static recrystallization; twin-roll casting; hot compression; magnesium alloy ZK60

1 Introduction

Magnesium numerous elements solute to form a series of magnesium alloys which have great potential for application in lightweight structural components due to their extremely low density, high specific strength and stiffness[1–3]. Moreover, wrought Mg alloys have attracted great attention in recent years owing to their higher mechanical properties than cast Mg alloys which usually have such casting defects as porosity, inclusions as well as low ductility[4–6]. At room temperature, however, their poor workability, strong preferred crystal orientation and mechanical properties directionality of wrought Mg alloys limit their extensive application from the automotive and aerospace industries to electronic devices and consumer products. All of these shortcomings were caused by their hexagonal crystallography and lack of sufficient independent slip systems. The activations of non-basal slip system such as prismatic and pyramid plane slip at evaluated temperature result in a gradually improved formability. Diverse hot work processes such as twin-roll casting (TRC), warm rolling (WR), hot extrusion (HE), torsion

straining (TS), reciprocal extrusion (RE) and equal channel angular extrusion (ECAE) are developed for the application of Mg alloys. TRC technology has such advantages as reducing several production steps in the production of strip and converting molten metals directly into an endless coiled strip suitable for cold rolling or wire-bars for wire-drawing. This technique has been developed continuously since it was first conceived by BESSEMER in 1856[7], which combines casting and hot rolling into a single step of flat rolled products. TRC processing reduces grain size and removes segregation. In addition, it saves cost due to a relatively high solidification rate ranging from 10² to 10³ K/s[8]. Despite of different hot work methods, the purpose of this study is to weaken basal texture, modify microstructure, refine grains and improve the mechanical properties. Due to the strong influence of grain size on the mechanical properties, grain refinement or coarsening prevention is a promising method to enhance the strength of wrought magnesium products[9–10], and progressive deformation of post-TRC materials is necessary. JEONG and HA[11] discussed the effects of rolling conditions on the microstructure and texture development of AZ31 Mg alloy sheet; CHEN et al[12] investigated the

microstructure and mechanical properties of AZ41 alloy sheets produced by twin roll casting, sequential warm rolling and post-annealing at 350 °C. However, the wrought materials possess high stored energy and a large fraction of non-equilibrium grain boundaries, which leads to the products non-stability in subsequent fabrication and application because of severe deformation [13–14]. Therefore, heat treatment methods were applied to induce dislocation rearrangement and accelerate the completion of recrystallization.

In the present work, the recrystallization of ZK60 alloy under TRC processing was studied. The microstructure evolutions at conventional casting (DC), twin roll casting (TRC) and hot compression (HC) were investigated. The effects of annealing on the microstructure and mechanical properties of ZK60 alloys under TRC-HC processing were discussed.

2 Experimental

Commercial magnesium alloy ZK60 was used and its chemical composition was Mg-6.20Zn-0.48Zr (mass fraction, %). The TRC processing was introduced in Ref. [15]. Uniaxial compression tests were performed with a strain rate of 0.1 s^{-1} at 350 °C, the schematic diagram of the TRC-HC processing was shown in Fig. 1. The specimens were quenched by nitrogen gas immediately after compression in order to prevent the microstructure from changing after deformation, then the samples were annealed at different temperatures (250–400 °C) and time (100–50 000 s). The annealed samples were mechanically polished with polycrystalline diamond suspension glycol based solution, and subsequently etched for 7 s with a solution of picric acid (5 g), acetic acid (5 mL), distilled water (10 mL) and ethanol (100 mL). All the optical microstructures were observed along the rolling direction; the average grain size was analyzed with image analyzer, and the hardness was measured with digital microhardness tester (TOKYO, MXT70) with a load of 100 g for 15 s. X-ray diffraction (XRD) analysis was done with a D/MAX-2000 equipment (RIGAKU). Microstructural evolution and grain boundary distributions were analyzed by electron backscatter diffraction (EBSD), the specimens were prepared by both mechanical using 2000# sand paper and electro polishing operated at 11 V for 120 s in a solution of 400 mL Butyl glycol, 80 mL ethanol and 40 mL perchloric acid (HClO_4) below 15 s to remove surface strain. EBSD data were acquired using a JEOL JSM-7001F field emission scanning electron microscope (FESEM) and HKL Channel 5 EBSD software (HKL Technology, Denmark). The FESEM was operated at 20 kV in high vacuum mode and the specimen was tilted at 70°.

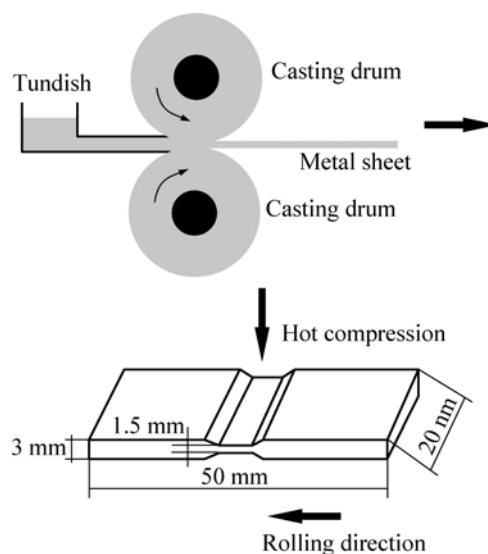


Fig. 1 Schematic diagram of TRC-HC processing

3 Results and discussion

3.1 Microstructures under different deformation condition

The optical images of ZK60 alloy deformed by DC, TRC and TRC-HC processing are shown in Fig. 2. For DC, coarse and equiaxed grains (100–200 μm) and some second eutectics as well as intermetallic compounds phases along the grain boundary and the interior of the grains were observed; for TRC, lots of dendrite structures were observed, phases separated out and embedded in the interdendritic region are much finer than the initial grains; twins are found in alloy after TRC, which were examined by EBSD technique as shown in Fig. 3. From orientation map, it can be seen that twins have various directions, from pole figure, the main twinning system is $\{10\bar{1}2\} 86.3^\circ <1\bar{2}10>$. The activation of extension twinning causes a misorientation of 86.3° between the twinned and the original part of crystal. Compared with the conventional casting, TRC processing has the advantages of improvement of microstructure modification and mechanical properties, it is shown that segregations are removed, grains are refined and microstructures are homogenized in Fig. 2(b). The same conclusions were deduced in Refs. [12, 16]. However, the microstructure characterizations of TRC-HC are distinctly different from that of DC and TRC. Significant microstructural changes indicated that TRC-HC processing is effective in refining grain size. From Fig. 2(c), distinct bimodal structures were observed, which consist of a large number of initial and deformed grains and a small number of newly formed grains. There are dynamic recrystallization (DRX), deformation bands (shear bands) and twins in the homogeneous and initial

grains. The shear bands look like long and wide “flowing rivers” which have about 37° tilting angle to the compression direction (Fig.2(c)). DRX-ed grains distribute in this “flowing rivers” while twins appear along the riverside, which results in distinct flow

softening. In addition, lots of sub-structures are studied in all the “river” and “riverside”.

The XRD patterns of ZK alloys after DC, TRC and TRC-HC processing are shown in Fig.4. The data were perpendicular to the normal direction (ND). Several

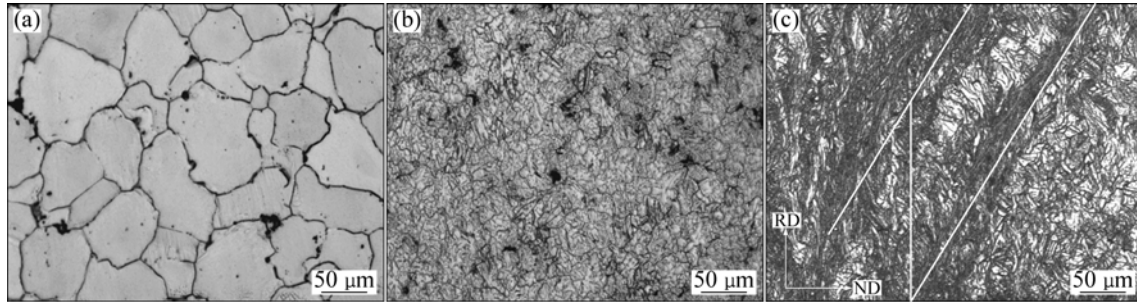


Fig.2 Optical images of ZK60 alloys under different processes: (a) DC; (b) TRC; (c) TRC-HC

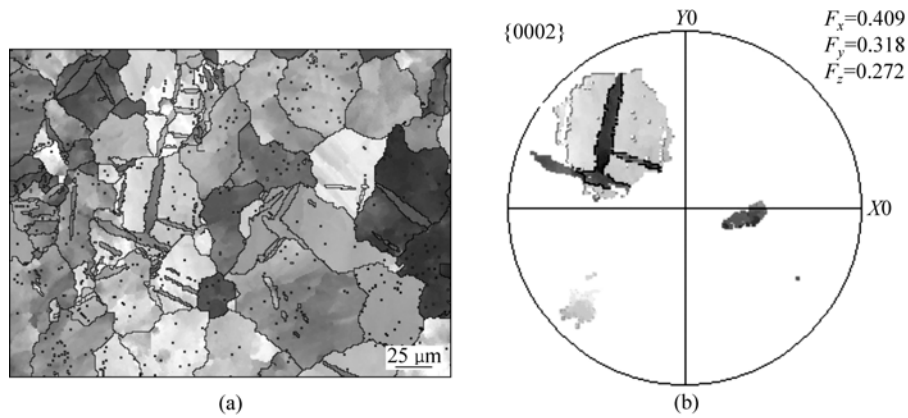


Fig.3 Twins in ZK60 alloy under TRC: (a) Orientation map; (b) Pole figure

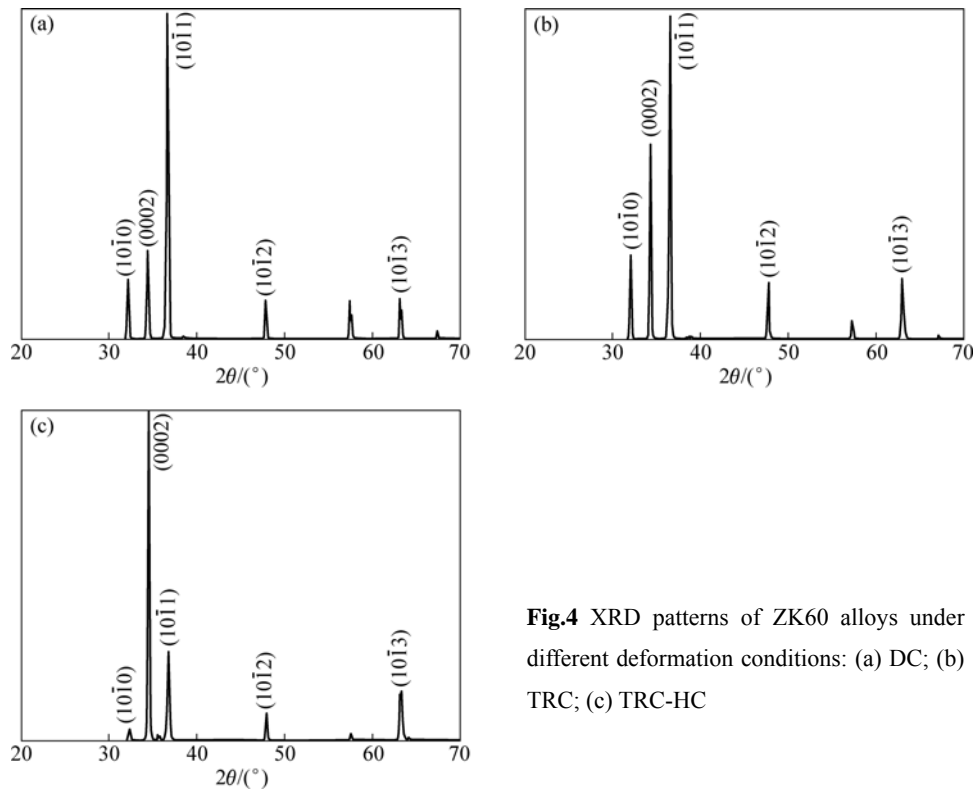


Fig.4 XRD patterns of ZK60 alloys under different deformation conditions: (a) DC; (b) TRC; (c) TRC-HC

important crystal planes, (0002), (10 $\bar{1}$ 0), (10 $\bar{1}$ 1), (10 $\bar{1}$ 2) and (10 $\bar{1}$ 3) are marked. Diffracted intensities of the main crystal planes, (0002), (10 $\bar{1}$ 0) and (10 $\bar{1}$ 1) are shown in Table 1. It is shown that the orientation of DC looks like random, TRC exhibits weak preferred orientation of hexagonal crystal structure, while TRC-HC exhibits strong basal texture orientation. With the increase of deformation degree, basal plane is gradually intensified, while the intensity of non-basal plane decreases. This indicates that with the increase of deformed degree, the sample develops a strong texture, and this causes the *c*-axes aligned in ND resulting in progressive basal plane orientation distribution. Other peaks such as (10 $\bar{1}$ 2) and (10 $\bar{1}$ 3) did not change distinctly, indicating that basal dislocation slips are the dominant deformation mode[17–18].

Table 1 Diffracted intensity of main planes in alloys in Fig.4

Plane	Intensity		
	CC	TRC	TRC-HC
(0002)	550	1 200	2 500
(10 $\bar{1}$ 0)	490	550	120
(10 $\bar{1}$ 1)	2500	1 950	700

3.2 Microstructures under different annealing conditions

EBSD Kikuchi band contrast maps for ZK60 alloys at deformation condition of 350 °C, 0.1 s⁻¹ and different annealing conditions are shown in Fig.5. The grey scales of band contrast maps are based on the relative intensity of the Kikuchi bands generated by the EBSD software. The dark region present the relatively low band contrast values caused by grain boundaries, particles and deformed features. The bright and white region present the occurrence of static recrystallization (SRX). It is clear that some recrystallized equiaxed grains decorate the shear bands, and elongated grains (non-shear banded materials) surround them. With the increase of annealing temperature, the amount of twins decrease while SRX grains increase; dislocations rearrange to form sub-grains. The low angle grain boundaries (LAGBs) continuously evolved into high angle grain boundaries (HAGBs), high proportions of HAGBs are consistent with high annealing temperature, while LAGBs are associated with severely deformed state as well as lower annealing temperature. Fig.6 shows the pole figure established

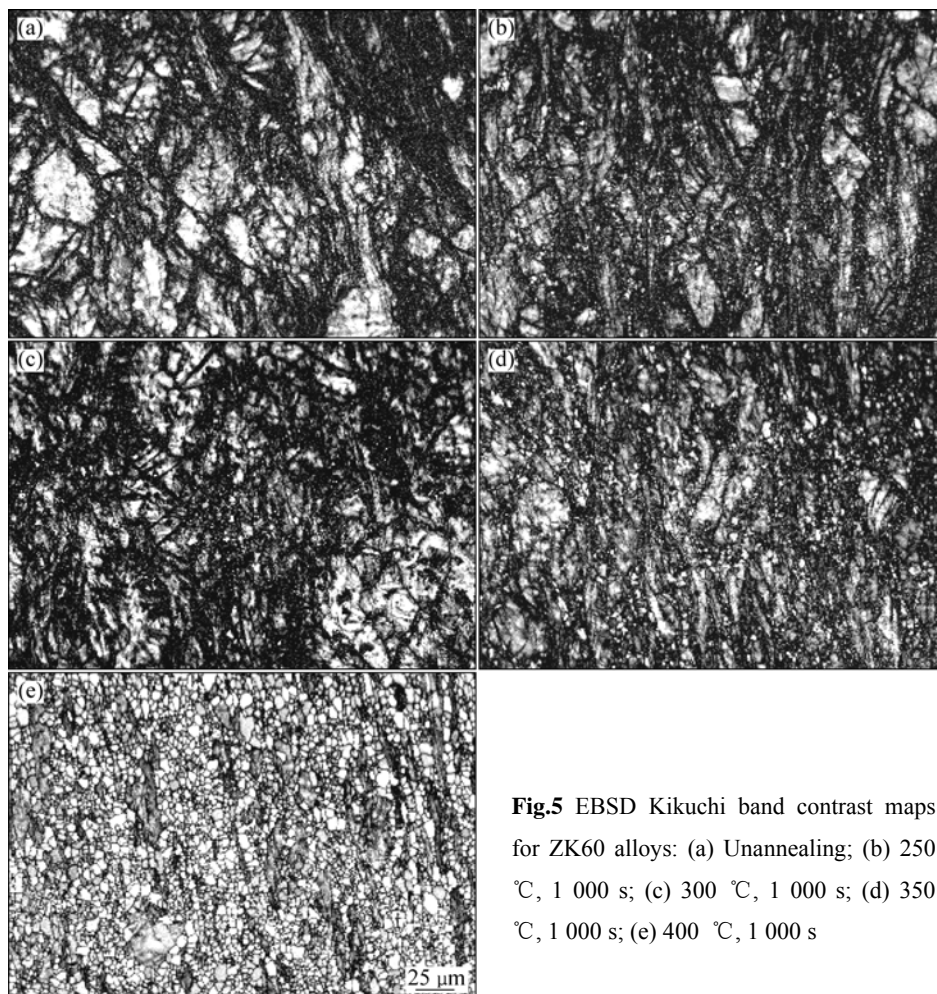


Fig.5 EBSD Kikuchi band contrast maps for ZK60 alloys: (a) Unannealing; (b) 250 °C, 1 000 s; (c) 300 °C, 1 000 s; (d) 350 °C, 1 000 s; (e) 400 °C, 1 000 s

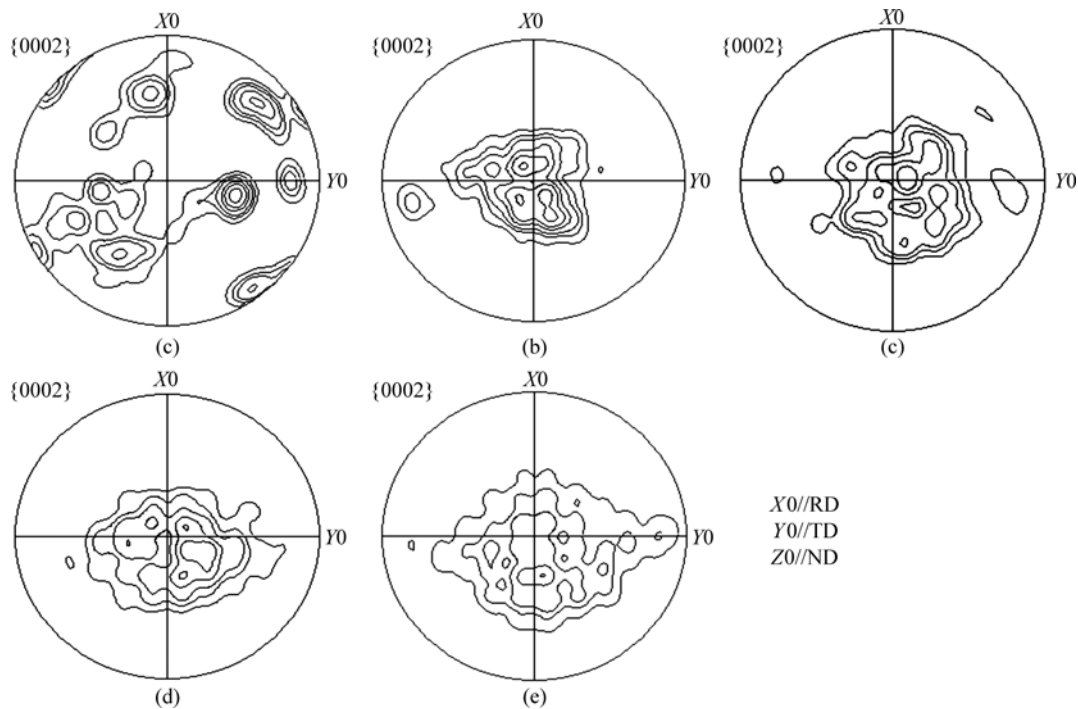


Fig.6 Pole figures established from EBSD data for ZK60 alloys (Contour levels: 1, 2, 3, 5, 7): (a) Unannealing; (b) 250 °C, 1 000 s; (c) 300 °C, 1 000 s; (d) 350 °C, 1 000 s; (e) 400 °C, 1 000 s

from EBSD data for ZK60 alloys at the deformation conditions of 350 °C, 0.1 s^{-1} and different annealing conditions. It is clear that the pivotal location of initial crystal orientation intensively influences the subsequent structural evolution. Under TRC-HC, the strong $\{0002\}$ basal plane orientation distribution is dominant although parts of DRX grains deviate from basal plane and align to $\{01\bar{1}0\}$ plane. Under annealing state, dislocation densities decrease with the increase of annealing temperature, the dark regions turn small, indicating that grain boundary turns clearer and twin boundary disappears.

3.3 Microhardnesses under different annealing conditions

Fig.7 shows the microhardness (H) changes as a function of annealing time (t) at different temperatures. The $H-t$ curves are divided into two regions (I and II). In Region I, the H values have no significant changes with the increase of annealing time and temperature. In Region II, there are two kinds of changes which can be divided into II_1 and II_2 regions. When $\theta < 300$ °C, there is a climbing trend with the increase of annealing time (II_2). When $\theta > 350$ °C, a degressive trend is obvious (II_1). This indicated that the dispersion strengthening particles improved the ability of softening resistance causing the improvement of hardness in II_2 stage, which is similar with the aging strengthening mechanism. At high temperature stage (II_1), grain size increases and the ductility improvement

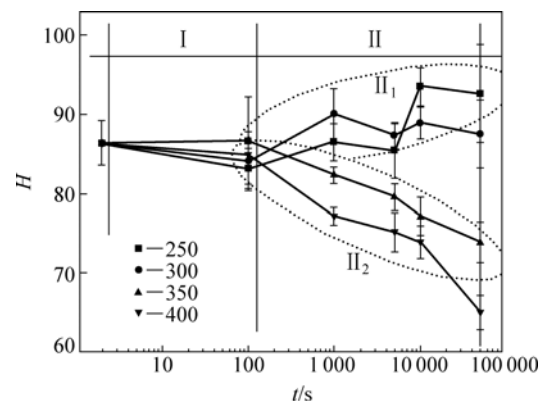


Fig.7 Microhardness as function of annealing time at different annealing temperature

results in decrease of hardness H .

It is well known that Hall–Petch (H–P) relationship is frequently reported to account successfully for the mechanical properties (strength and hardness) dependence of the grain size of structural element:

$$H = H_0 + k_H d^{-n} \quad (1)$$

where H is the hardness; d is the average size of grains; k_H and n are called H–P parameters; H_0 is the initial hardness of pre-annealing. Both parameters k_H and n reflect the resistance of the boundary to dislocation glide. In regard to the severe deformation ZK60 alloys of subsequent annealing time and temperature is important for SRX, that is, annealing parameters are crucial in the microstructural evolution from substructure to stable

structure. Thus, $n=1$ is valid for sub-grain boundaries of deformed materials. Whereas overfull annealing time and super high temperature result in the growth of recrystallized grains to high angle boundaries, under this condition, $n=1/2$. Therefore, the H - P relationship can be described as

$$H=H_{01}+k_{H1}d^{-1/2} \quad (2)$$

$$H=H_{02}+k_{H2}d^{-1} \quad (3)$$

where H_0 and k_H are calculated by the $H-d^{-1/2}$ relationship in Fig.8; k_H is the slope of H - P line; $k_{H1}=80$; $k_{H2}=150$; H_0 is the intercept; $H_{01}=69$, $H_{02}=55$. It can be deduced that H_0 and k_H are related to not only the material variety but also the deformation degree.

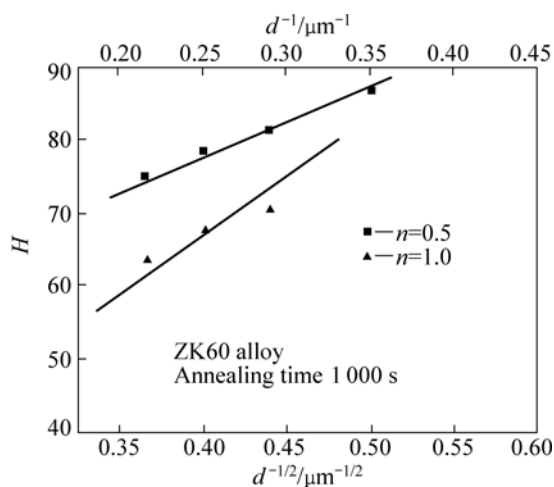


Fig.8 Hall–Petch relationship for ZK60 alloys

4 Conclusions

1) Twin roll casting possesses weak preferred orientation of hexagonal crystal structure while TRC-HC exhibits strong basal texture orientation. With the increase of annealing temperature, the amount of twins decreases while SRX grain increases. Dislocations rearrangement form sub-grains ultimately induced static recrystallization.

2) Different annealing conditions affect the microstructural evolution and microhardness. Shortening annealing time has a small effect on hardness. Longer time at lower annealing temperature results in the increases of the hardness, while higher annealing temperature causes the decrease of the hardness.

References

[1] FU Peng-huai, PENG Li-ming, JIANG Hai-yan, CHANG Jian-wei, ZHAI Chun-quan. Effects of heat treatments on the microstructures And mechanical properties of Mg-Nd-Zn-Zr alloy [J]. Mater Sci Eng A, 2008, 486: 183–192.

[2] STANFORD N, BARNETT M R. The origin of “rare earth” texture development in extruded Mg-based alloys and its effect on tensile

ductility [J]. Mater Sci Eng A, 2008, 496: 399–408.

[3] LUO Shou-jing, SHAN Wei-wei. Steady state rheological behavior of semi-solid ZK60-RE magnesium alloy during compression [J]. Transactions of Nonferrous Metals Society of China, 2007, 17(5): 974–980.

[4] SONG S X, HORTON J A, KIM N J, NIEH T G. Deformation behavior of a twin-roll-cast Mg-6Zn-0.5Mn-0.3Cu-0.02Zr alloy at intermediate temperatures [J]. Scripta Materialia, 2007, 56(5): 393–395.

[5] WANG G Y, WANG X J, CHANG H, WU K, ZHENG M Y. Processing maps for hot working of ZK60 magnesium alloy [J]. Mater Sci Eng A, 2007, 464(1/2): 52–58.

[6] GALIYEV A, KAIBYSHEV R, GOTTSTEIN G. Correlation of plastic deformation and dynamic recrystallization in magnesium alloy ZK60 [J]. Acta Mater, 2001, 49: 1199–1207.

[7] WATARI H, DAVEY K, RASGADO M T, HAGA T, IZAW S. Semi-solid manufacturing process of magnesium alloys by twin-roll casting [J]. Journal of Materials Processing Technology, 2004, 155/156: 1662–1667.

[8] YANG Xu-yue, JI Ze-sheng, MIURA H, SAKAI T. Dynamic recrystallization and texture development during hot deformation of magnesium alloy AZ31 [J]. Transactions of Nonferrous Metals Society of China, 2009, 19(1): 55–60.

[9] BUHA J. The effect of micro-alloying addition of Cr on age hardening of an Mg–Zn alloy [J]. Mater Sci Eng A, 2008, 492(1/2): 293–299.

[10] GARCES G, MULLER A, ONORBE E, PEREZ P, ADEVA P. Effect of hot forging on the microstructure and mechanical properties of Mg-Zn-Y alloy [J]. Journal of Materials Processing Technology, 2008, 206(1/3): 99–105.

[11] JEONG H T, HA T K. Texture development in a warm rolled AZ31 magnesium alloy [J]. Journal of Materials Processing Technology, 2007, 187/188: 559–561.

[12] CHEN Hong-mei, KANG Suk-bong, YU Hua-shun, KIM Hyoung-wook, MIN Guang-hui. Microstructure and mechanical properties of Mg-4.5Al-1.0Zn alloy sheets produced by twin roll casting and sequential warm rolling [J]. Mater Sci Eng A, 2008, 492(1/2): 317–326.

[13] TAKAYAMA A, YANG X, MIURA H, SAKAI T. Continuous static recrystallization in ultrafine-grained copper processed by multi-directional forging [J]. Mater Sci Eng A, 2008, 478(1/2): 221–228.

[14] HUMPHREYS F J, HATHERLY M. Recrystallization and related annealing phenomena [M]. 2nd ed. Kidlington, UK: Elsevier, 2004: 118–123.

[15] KANG S B, CHO J H, KIM H W, JIN Y M. Effect of heat treatment on microstructure and mechanical properties in ZK60 alloy sheet [J]. Materials Science Forum, 2008, 567/568: 361–364.

[16] EDDAHBI M, DEL VALLE J A, PEREZ-PRADO M T, RUANO O A. Comparison of the microstructure and thermal stability of an AZ31 alloy processed by ECAP and large strain hot rolling [J]. Mater Sci Eng A, 2005, 410/411: 308–311.

[17] ZUBEROVA Z, ESTRIN Y, LAMARK T T, JANECEK M, HELLMIG R J, KRIEGER M. Effect of equal channel angular pressing on the deformation behaviour of magnesium alloy AZ31 under uniaxial compression [J]. Journal of Materials Processing Technology, 2007, 184(1/3): 294–299.

[18] LIBOR HELIS, KAZUTO OKAYASU, HIROSHI FUKUTOMI. Microstructure evolution and texture development during high-temperature uniaxial compression of magnesium alloy AZ31 [J]. Mater Sci Eng A, 2006 430: 98–103.

(Edited by FANG Jing-hua)